Chapter 19
ROESY

Ad Bax and Stephan Grzesiek

National Institutes of Health, DHHS NIDDK LCP, Building 5, Room 126, 9000 Rockville Pike, Bethesda, MD 20892-0520, USA

19.1 INTRODUCTION

Molecular motion in liquids results in a time dependence of the dipolar coupling between two spins, which gives rise to transitions between the nuclear spin states. These transitions constitute the basis of the nuclear Overhauser enhancement (NOE) effect, which has long been one of the NMR cornerstones for the study of molecular structure.[1] As discussed in Chapter 18, the transition rates are determined by the square of the dipolar coupling, i.e., by r^{-6}, where r is the internuclear distance, by the angular Larmor frequency ω_0, and by the decay constant τ_c of the autocorrelation function of the time-dependent dipolar coupling $D(t)$. In conventional homonuclear NOE experiments, the change in z magnetization of a spin B is monitored after the z magnetization of a spin A in its immediate vicinity has been perturbed. Provided τ_c is known, the rate at which the longitudinal magnetization of spin B changes after perturbing the z magnetization of A provides a measure of r. For $\omega_0\tau_c < 1.12$, the z magnetization of spin B will increase to a value higher than its Boltzmann equilibrium value when saturating the resonance of A (positive NOE), whereas the opposite holds for $\omega_0\tau_c > 1.12$. For many interesting molecules of intermediate size (500–2000 Da), the product $\omega_0\tau_c$ is frequently found to be close to 1, resulting in very small NOE effects.

As outlined above and described in detail elsewhere,[1–4] the NOE is a cross-relaxation effect between longitudinal components of nuclear spin magnetization. In 1983, Bothner-By and co-workers developed a different type of NOE experiment, which measures cross relaxation between magnetization components that are perpendicular to the static magnetic field.[5] The original name of this experiment is *c*ross relaxation *a*ppropriate for *m*inimolecules *e*mulated by *l*ocked *s*pins, or CAMELSPIN, but it is more commonly known as ROESY, for *r*otating-frame *O*verhauser *e*nhancement *s*pectroscopy. As implied in the original acronym of this experiment, the transverse cross relaxation is positive for all values of the rotational correlation time, i.e., it is the same as that found for small molecules in the NOESY experiment. The original

motivation for this experiment was to study the structure of intermediate size molecules, which have near-zero longitudinal NOE effects. However, as pointed out in the original report,[5] the positive sign of the ROE effect also allows one immediately to distinguish cross relaxation from chemical exchange effects, which are always negative. This latter application has proven critical, for example, in studying hydration of proteins.[6,7] Other important applications lie in the area of macromolecular structure determination, where the rotating frame Overhauser enhancement, owing to its positive sign, tends to be far less susceptible to spin diffusion effects than its longitudinal counterpart.[8,9] Although for macromolecules, the inherent sensitivity of the ROESY experiment is less than for NOESY, numerous useful applications to proteins and nucleic acids have been reported. In addition to the nonselective ROESY experiment, a number of very interesting selective variants have been developed that can selectively probe small subsets of the Redfield cross-relaxation matrix. These elegant ROESY variants are particularly powerful for probing cross correlation,[10–12] and they have been treated and reviewed in great detail by Bull.[13] The discussion below is restricted to the more commonly used nonselective ROESY experiments and their various applications.

19.2 PRINCIPLES OF ROTATING FRAME OVERHAUSER SPECTROSCOPY

The state of a spin system is most conveniently described by the density matrix $\hat{\rho}$. For a system of two spin-$^1/_2$ nuclei, A and X, $\hat{\rho}$ is a simple 4×4 matrix. Its diagonal elements, ρ_{11}, ρ_{22}, ρ_{33}, and ρ_{44} correspond to the populations of energy levels 1, . . . , 4. An off-diagonal element such as ρ_{12} represents the coherence or transition between levels 1 and 2, etc. In order to describe relaxation phenomena, the Hamiltonian is usually split into a spin-dependent part $\hat{\mathcal{H}}_S$ and a spin–lattice coupling $\hat{\mathcal{H}}_{SL}$. The spin-dependent component $\hat{\mathcal{H}}_S$ consists of the Zeeman coupling to the main external magnetic field ($\hat{\mathcal{H}}_0$) plus other, much smaller, purely spin-dependent components ($\hat{\mathcal{H}}_1$) such as chemical shift, J coupling, and coupling of the spins to radiofrequency (rf) fields. The spin–lattice part $\hat{\mathcal{H}}_{SL}$ describes the coupling of the spins to the external heat bath, which is a stochastic process. Transformation into the interaction frame makes the Zeeman term $\hat{\mathcal{H}}_0$ disappear in explicit form from the Hamiltonian, and hides it as a time dependence of the operators and the density matrix. In this interaction frame and under a number of approximations, the time dependence of the density matrix $\hat{\rho}$ is then described by

$$\frac{\mathrm{d}\hat{\rho}(t)}{\mathrm{d}t} = -\mathrm{i}[\hat{\mathcal{H}}_1, \hat{\rho}] - \hat{R}\hat{\rho} \qquad (19.1)$$

$\hat{R}$ is the Redfield relaxation matrix, which describes the return to equilibrium of the spin system. A product $R_{12\ 13}\rho_{13}$, for example, describes the loss per unit time of the density matrix element ρ_{12} caused by the matrix element ρ_{13}. It is important to realize, however, that relaxation is usually a slow process relative to evolution under the static Hamiltonian. Consequently, cross relaxation can only occur if the off-diagonal elements ρ_{12} and ρ_{13} oscillate at nearly the same frequencies in the laboratory frame, i.e., if the corresponding resonances overlap. In this case, the cross relaxation between the 1–2 and the 1–3 transitions is termed a secular process. If their frequencies are different, the exchange of magnetization is a nonsecular process, and can be neglected. ROESY and its selective variants all rely on modifying the spin Hamiltonian $\hat{\mathcal{H}}_1$ in such a manner that cross relaxation can be probed between transitions that would differ in frequency in the absence of radiofrequency irradiation. In the standard ROESY experiment, this is accomplished simply by the application of a strong monochromatic rf field, which locks all magnetization that is parallel to it and dephases any perpendicular components. Neglecting off-resonance effects, the cross-relaxation rate for magnetization components locked along the rf field is therefore identical to the cross relaxation between the transverse magnetization components of two exactly overlapping resonances (identical spins).

Following Bothner-By *et al.*,[5] the time dependence of the spin locked magnetization components m_A and m_B of two homonuclear spins A and B is described by

$$\frac{\mathrm{d}m_A(t)}{\mathrm{d}t} = -R_{2A}m_A(t) - R_{AB}m_B(t) \quad (19.2a)$$

$$\frac{\mathrm{d}m_B(t)}{\mathrm{d}t} = -R_{AB}m_A(t) - R_{2B}m_B(t) \quad (19.2b)$$

where R_{AB} is the cross-relaxation rate of interest, and R_{2A} and R_{2B} are the autorelaxation rates, describing the loss of magnetization, which also includes processes other than cross relaxation between spins A

and B. For convenience, we assume below that $R_{2A} = R_{2B} = R_2$, which results in a particularly simple solution of equations (19.2a) and (19.2b). If two experiments are done, one with $m_A(0) = m_B(0) = 1$ and one with $m_A(0) = -m_B(0) = 1$ (for example, by selectively inverting the magnetization of spin B immediately prior to a nonselective 90°_x pulse, which is followed by a *y*-axis spin lock), the time dependence of $m_A(t)$ and $m_B(t)$ in these two cases is given by

$$\begin{aligned} m_A(t) &= m_B(t) \\ &= \exp[-(R_2 + R_{AB})t] \qquad (19.3a) \\ m_A(t) &= -m_B(t) \\ &= \exp[-(R_2 - R_{AB})t] \qquad (19.3b) \end{aligned}$$

The difference between equations (19.3a) and (19.3b) represents the ROE, which has a maximum value for

$$t = \frac{1}{2R_{AB}} \ln \frac{R_2 + R_{AB}}{R_2 - R_{AB}} \qquad (19.4)$$

In the isolated spin pair approximation, R_2 and R_{AB} are given by

$$\begin{aligned} R_2 = {} & \frac{\gamma^4 h^2 (\mu_0/4\pi)^2}{80\pi^2 r^6} \\ & \times [5J(0) + 9J(\omega_0) + 6J(2\omega_0)] \qquad (19.5) \end{aligned}$$

$$R_{AB} = \frac{\gamma^4 h^2 (\mu_0/4\pi)^2}{80\pi^2 r^6} [4J(0) + 6J(\omega_0)] \qquad (19.6)$$

where r is the internuclear distance and, for protons, $\gamma^4 h^2 (\mu_0/4\pi)^2/80\pi^2 = 2.84 \times 10^{10}\ \mathrm{s^{-2}\AA^6}$. The reduced spectral density function $J(\omega)$ for isotropically reorienting molecules is defined as

$$J(\omega) = \frac{\tau_c}{1 + \omega^2 \tau_c^2} \qquad (19.7)$$

The maximum Overhauser enhancement obtainable for this isolated two-spin pair, using the ROE mixing time of equation (19.4), is shown graphically in Figure 19.1(a). In practice, the isolated spin pair approximation is usually not valid, and frequently R_2 is much larger than R_{AB}. In this case, it follows from equation (19.4) that the maximum ROE effect is obtained for

$$t \approx 1/R_2 \qquad (19.8)$$

which means that the highest sensitivity is obtained for a mixing period on the order of the transverse relaxation time T_2, as measured, for example, by a selective spin echo experiment.

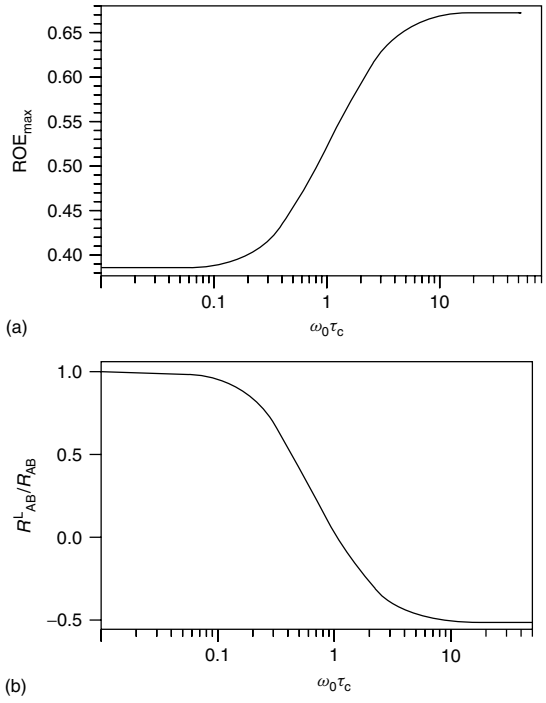

Figure 19.1. (a) Maximum obtainable ROE enhancement ROE_{max} in the isolated two-spin pair approximation, assuming that the spins are relaxed exclusively by homonuclear dipolar interactions. (b) The ratios of the cross relaxation rates in the laboratory frame, R^L_{AB}, and in the rotating frame, R_{AB}, as functions of $\omega_0\tau_c$.

19.3 COMPARISON WITH LABORATORY FRAME NOE

In the isolated spin pair approximation and assuming rigid body motion, comparison of the ROE and NOE results is straightforward. The ROE build-up rate follows directly from equation (19.6), and the analogous cross-relaxation rate in the laboratory frame is given by

$$R^L_{AB} = \frac{\gamma^4 h^2 (\mu_0/4\pi)^2}{40\pi^2 r^6} [6J(2\omega_0) - J(0)] \qquad (19.9)$$

Figure 19.1(b) shows the ratio of the cross-relaxation rates in the laboratory and rotating frames as a function of $\omega_0\tau_c$. For $\omega_0\tau_c \ll 1$, the build-up rates are nearly identical, whereas in the slow motion limit ($\omega_0\tau_c \gg 1$) R_{AB} approaches $-2R^L_{AB}$. Because of the dependence of R^L_{AB}/R_{AB} on $\omega_0\tau_c$, this ratio in principle can be used directly to determine the rotational

correlation time τ_c, allowing one to derive absolute interproton distances from either R^L_{AB} or R_{AB}.[14] In practice, the use of this approach is limited to the region $0.3 < \omega_0\tau_c < 3$, where the ratio R^L_{AB}/R_{AB} has its steepest dependence on τ_c. A second potential problem with this approach is caused by rapid internal motion, such as methyl group rotation, which also affects R^L_{AB}/R_{AB}.[15]

19.3.1 Sensitivity Considerations

Although the cross-relaxation rate in the rotating frame is always higher than in the laboratory frame, this does not mean that the sensitivity of the ROESY experiment is always greater than for NOESY. The relative sensitivity of the two experiments can be derived by calculating the spectra obtained for mixing times that maximize the cross-peak intensity. As seen from equation (19.4), for the ROESY experiment this optimum mixing time depends on the transverse magnetization leakage rate R_2, and for the NOESY experiment it depends on the longitudinal leakage rate R_1. Neglecting the effect of the different NOESY and ROESY mixing times on the total duration of each experiment, the sensitivity ratio ξ of the NOESY versus the ROESY experiment has been calculated by Farmer *et al.*[15,16] for two different external relaxation rates R_{ext}, and is shown in Figure 19.2. This figure suggests that the ROESY experiment is expected to yield higher sensitivity than the NOESY experiment over a wide range of rotational correlation times. There are several practical reasons that reduce the sensitivity advantage of ROESY over NOESY, however. For example, off-resonance effects reduce the cross-relaxation rate in the ROESY experiment,[10,14–17] and so do spurious coherent Hartmann–Hahn magnetization transfer processes,[18] both discussed in some more detail below. Also, Figure 19.2 assumes that the external relaxation contribution R_{ext}, which represents the leakage rate from mechanisms other than homonuclear dipolar interactions, is identical for R_1 and R_2. For macromolecules, this approximation may not be valid, since proton chemical shift anisotropy and heteronuclear dipolar coupling have far larger effects on R_2 than on R_1. For $\omega\tau_c > 1.12$, there also is a third reason: because of the negative sign of the NOE, indirect contributions to the NOE cross peak increase its intensity. The opposite holds for the ROESY experiment, where the positive sign of the ROE causes the indirect contribution, relayed via one spin, to be opposite in sign to the direct contribution (the so-called three-spin effect). Indirect contributions therefore attenuate the cross-peak intensity in the ROESY spectrum and, for $\omega_0\tau_c > 1.12$, they increase the cross-peak intensity in NOESY.

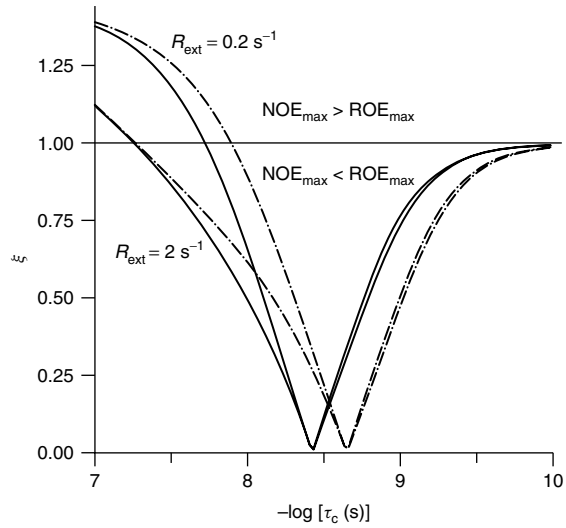

Figure 19.2. The ratio of the maximum cross-peak magnitude for NOESY compared with ROESY, ξ, as a function of the rotational correlation time τ_c for an AX spin system with interatomic distance $r_{AX} = 0.3$ nm. Plots are shown for Larmor frequencies of 300 MHz (–) and 500 MHz (·–·–·) and for two different external relaxation rates R_{ext}. R_{ext} represents contributions to the leakage rate from sources other than homonuclear dipolar interactions. R_{ext} was assumed to be independent of τ_c, and identical for NOESY and ROESY. Reproduced, with permission, from Farmer *et al.*[15]

19.3.2 The Effect of Internal Motion

In both the NOESY and ROESY experiments, cross-relaxation and leakage rates are strongly influenced by rapid internal motions. These internal motions change the shape of the spectral density function and constitute a major obstacle when attempting to derive accurate internuclear distances from the cross relaxation rates. In the model-free approach for rapid internal motion,[19,20] the spectral density function $J(\omega)$ becomes

$$J(\omega) = \frac{S^2\tau_c}{1+\omega^2\tau_c^2} + \frac{(1-S^2)\tau}{1+\omega^2\tau^2} \qquad (19.10)$$

where S^2 is the generalized order parameter, τ_c is again the molecular rotational correlation time, and $1/\tau = 1/\tau_e + 1/\tau_c$, with τ_e the effective correlation time of any internal motions. If S^2 and τ_e are known, equation (19.10) can be substituted directly into equation (19.6). In practice, however, detailed knowledge of S^2 and τ_e is rarely available. Note that S^2 would need to be known for every proton pair; assuming 'rigid' protons A and X and a third proton M, subject to restricted internal mobility, the order parameters for A–M and M–X interactions are likely to have different values. However, it is clear from equations (19.6) and (19.10) that rapid internal motion ($\omega_0\tau_e \ll 1$) reduces the rotating frame cross-relaxation rate. When using only a single mixing time for estimating the ROE cross-relaxation rate, the error in the linear build-up approximation also reduces the rotating frame cross-relaxation rate. Provided τ_c is known, measurement of R_{AB} therefore yields an upper limit distance constraint that is at least as large as the true interproton distance, and the errors merely weaken the constraint that is being used. In contrast, indirect NOE effects (spin diffusion) can be a major problem when using NOESY to study macromolecular conformation, since they can result in a very significant underestimate of the upper limit for the interproton distance. Such an underestimate can actually result in distorted structures.

Because of the positive sign of the ROE, indirect ROE effects generally result in a reduction in cross-peak intensity, or even in a sign change (three-spin effect), which does not result in too tight a distance constraint. As a rule of thumb, interproton distances larger than 0.35 nm rarely give rise to observable ROE cross peaks. This can, of course, also be considered to be a disadvantage, since it results in a much smaller set of interproton distance constraints. It has been suggested that for protein structure determination, the number of constraints is more important than their precise values.[21]

19.3.3 Equivalent Spins

Farmer *et al.*[15] provide a detailed discussion of the effect of equivalent spins on NOE and ROE cross-relaxation and leakage rates. For methyl groups, for example, they show that the very rapid cross relaxation among the equivalent methyl protons can lead to a dramatic increase in the leakage rate, which adversely affects the maximum obtainable ROESY cross-peak intensity. Note that intramethyl group cross relaxation does not contribute to the leakage term in the NOESY experiment. In the absence of rapid methyl group rotation and for long τ_c values (>30 ns), the maximum obtainable ROESY intensity becomes more than an order of magnitude less sensitive than for NOESY. Rapid methyl group rotation ($\tau_e < 1$ ns) quenches the intramethyl group cross relaxation, however, and NOESY and ROESY are then again of comparable sensitivity.[15] In contrast to methyl groups, methylenes are not usually subject to extensive internal dynamics, resulting in a high leakage rate in the slow tumbling limit. Cross peaks reach a maximum intensity for short mixing times, and the sensitivity of the ROESY experiment is reduced.

19.4 EXPERIMENTAL REALIZATION

A variety of different experimental schemes have been proposed for recording ROESY spectra. Some of the more popular ones are sketched in Figure 19.3, and these are briefly discussed below. The pulse schemes of Figure 19.3(a) and (b) are the original 1D and 2D methods for recording CAMELSPIN/ROESY spectra.[5] In (a), a selective 180° pulse inverts the z magnetization of a preselected resonance on alternate scans. After a subsequent 90°_x pulse, a strong monochrome radiofrequency field (SL_y) locks the spins along the y axis, and cross relaxation takes place. Subtracting odd- from even-numbered transients, recorded with and without selective inversion of the preselected resonance, yields the 1D difference spectrum, which shows intensity for spins that cross relax with the inverted spin. Figure 19.3(b) is the simple 2D analog of the 1D experiment, where frequency labeling is accomplished by a 90° pulse followed by the variable evolution period t_1, instead of the selective pulse.

As discussed below, for minimizing homonuclear Hartmann–Hahn transfer (see Chapter 20) during the application of the spin lock field, it is necessary that the effective spin lock fields for J coupled spins be different.[18] This can be accomplished either by using a relatively weak rf field strength or by positioning the rf carrier at one side of the spectrum. In this case, the effective field makes an angle θ with the z axis, and only a fraction $\sin\theta \cos\omega_A t_1$ of the A-spin magnetization is locked along the effective

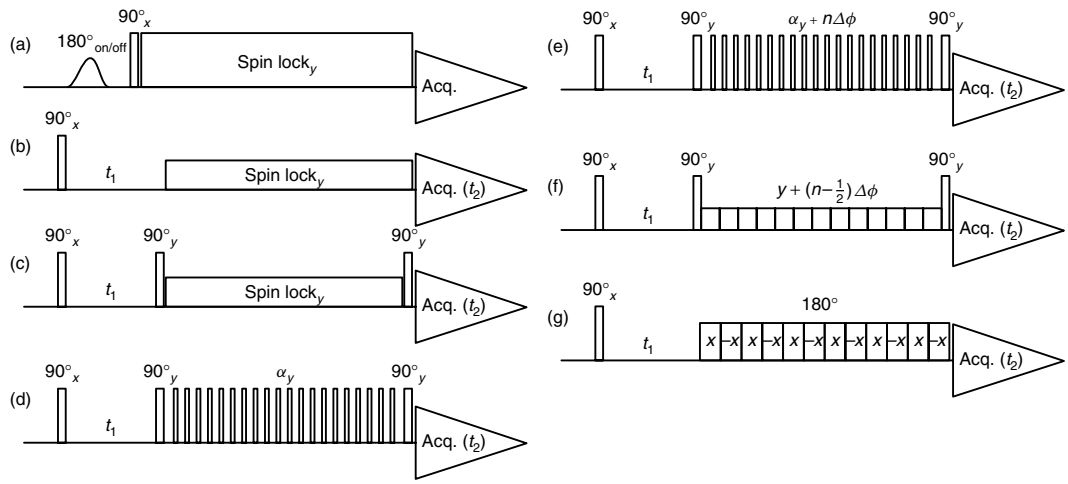

Figure 19.3. Experimental schemes for recording ROESY spectra. (a) One-dimensional scheme. (b) Original two-dimensional scheme. (c) Scheme with 90°_y pulses bracketing the y axis spin lock, to avoid signal loss caused by off-resonance spin locking. (d) Spin lock with small-angle ($\alpha \approx 30^\circ$) pulses, separated by short delays, and bracketing pulses. (e) Spin lock with phase ramping of the α pulses. If $N\ \Delta\phi = 2\pi$, the total number of α pulses needs to be an integral multiple of N. The delay between the 90°_y and the first α pulse, and between the last α pulse and the following 90°_y pulse, needs to be half the duration of the α pulse spacing τ_d. Phase ramping merely serves to obtain the same effect as moving the carrier by $\Delta\phi/(\tau_p + \tau_d)$, where τ_p is the duration of the α pulse, from its actual position during the spin lock, without introducing problems related to phase continuity. (f) Same as (e), but using a continuous spin lock. (g) Transverse spin lock, where the spins are 'locked' along an axis perpendicular to the axis (x) along which the pulses are applied. For minimizing homonuclear Hartmann–Hahn contributions, the carrier position and rf amplitude need to be adjusted for schemes (a)–(d), and the phase-ramp-generated offset needs to be adjusted for schemes (e) and (f). To avoid excessive sample heating, the power used during the mixing period in schemes (e)–(g) may also need to be reduced. For the 2D schemes (b)–(g), quadrature in F_1 is obtained by changing the phase of the first pulse in the standard States,[22] TPPI,[23] or States–TPPI[24] manner.

field (Figure 19.4), where ω_A is the angular resonance frequency of spin A. After the spin lock field is turned off, only a fraction $\sin\theta$ of the spin locked magnetization is present in the transverse plane, and the sensitivity of the experiment is effectively reduced by $\sin^2\theta$. This off-resonance loss can be avoided if the weaker spin lock field is bracketed by nonselective 90°_y pulses (Figure 19.3c).[25] In this case, a fraction $\sin(\omega_A t_1 + \theta)$ of the transverse A-spin magnetization will be spin locked along the effective field. At the end of the ROESY mixing period, all spin locked magnetization is returned to the transverse plane by the final 90°_{-y} pulse. The loss in signal by a factor $\sin^2\theta$, as applies to the scheme in Figure 19.3(b), is now transferred into a phase error θ in both the F_1 and F_2 dimensions of the spectrum. To a good approximation, the phase error θ depends linearly on the resonance offset, and a first-order frequency-dependent phase correction can be used to compensate for it. Note that no phase cycling of the 90°_y pulses relative to the y axis spin lock should be used, since inverting the phase of this pulse to 90°_{-y} would also invert the phase error. Co-adding the spectra would then remove the phase error and reintroduce the amplitude loss.

The use of a low-power spin lock mixing period requires the capability to rapidly change the rf power level, which may constitute a problem on older spectrometers. This problem can be avoided by replacing the continuous spin lock by a series of closely spaced high-power pulses (Figure 19.3d), each of a small flip angle ($\sim 30^\circ$).[26] If the flip angle of the short pulse is α, and M pulses are applied per second, this irradiation is equivalent to spin locking with a continuous rf field of $M\alpha/2\pi$ (in Hz), provided that M (in Hz) $\gg \delta_{max}$, where δ_{max} is the maximum offset of a resonance of interest from the rf carrier frequency. Relative to a continuous rf field of equivalent field strength, the use of small flip angle

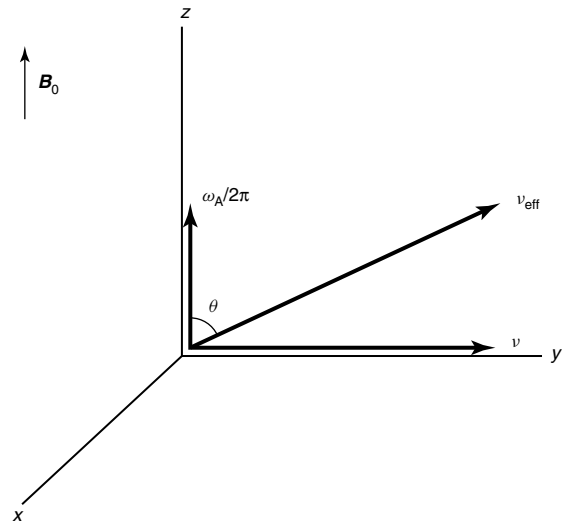

Figure 19.4. Definition of the effective field direction ν_{eff} for spin A at resonance offset $\omega_A/2\pi$, during irradiation with an rf field of strength ν along the y axis. Before the spin lock field is turned on, the transverse magnetization of A, $\boldsymbol{M}_A$, is in the (x,y) plane.

pulses does not reduce the amount of undesirable homonuclear Hartmann-Hahn cross polarization[17]. If the pulse spacing is τ_d and the pulse duration is τ_p, the pulsed spin lock increases the average power used during spin lock by $(\tau_d + \tau_p)/\tau_p$ over a continuous spin lock of the same effective field strength. In some situations, this can lead to undesirable sample heating effects. The $\sin^2\theta$ signal loss that occurs in the scheme of Figure 19.3(b) also applies to a series of small flip angle α pulses, and this problem can again be corrected by the application of two 90°_y bracketing pulses (Figure 19.4d).

19.5 MINIMIZATION OF J CONTRIBUTIONS

Coherent magnetization transfer, primarily via zero quantum coherence, has been a major nuisance in NOESY spectra (see Chapter 18), where it gives rise to antiphase cross peaks of zero integrated intensity.[2,3,27] A similar problem exists in ROESY, where there are actually two distinct mechanisms for coherent transfer of magnetization between J-coupled spins: COSY and HOHAHA (see Chapter 16).

19.5.1 COSY Artifacts in ROESY

Considering the simplest 2D scheme of Figure 19.3(b), the experiment can also be considered as a COSY experiment[28] with a very long mixing pulse. During the evolution period t_1, A-spin magnetization becomes antiphase with respect to its coupling partner, X, and is subsequently transferred by the spin lock pulse, of total flip angle β, into antiphase X spin magnetization. In product operator terms,

$$\begin{aligned}\hat{A}_y &\xrightarrow{t_1} \cos(\pi J_{AX} t_1)\hat{A}_y - 2\sin(\pi J_{AX} t_1)\hat{A}_x\hat{X}_z \\ &\xrightarrow{\beta_y} +2\sin^2\beta\sin(\pi J_{AX} t_1)\hat{A}_z\hat{X}_x + \ldots \quad (19.11)\end{aligned}$$

Even though β varies spatially over the sample owing to rf inhomogeneity, $\sin^2\beta$ does not average to zero. However, with neither spin A nor X on resonance, the effective rf fields experienced by the two spins, ν_{effA} and ν_{effX}, will always be stronger than the nominal rf field strength ν:

$$\begin{aligned}\nu_{\text{effA}} &= \nu\left(1+\frac{\delta_A^2}{\nu^2}\right)^{1/2} \approx \nu + \frac{\delta_A^2}{2\nu} \\ \nu_{\text{effX}} &= \nu\left(1+\frac{\delta_X^2}{\nu^2}\right)^{1/2} \approx \nu + \frac{\delta_X^2}{2\nu} \quad (19.12)\end{aligned}$$

where δ_A and δ_X are the offsets of spins A and X. The effective flip angles β_A and β_X experienced by each of the two spins will therefore differ, and the term $\sin^2\beta$ must be rewritten as $\sin\beta_A \sin\beta_X$, and this product averages to zero when $(\delta_A{}^2 - \delta_X{}^2)\tau/2\nu$ varies rapidly over the sample volume, where τ is the duration of the spin lock period. COSY-type artifacts in ROESY spectra can therefore be minimized by

1. selecting the carrier position judiciously, to maximize $\delta_A^2 - \delta_X^2$,
2. using a relatively weak spin lock field strength ν, and
3. using a long mixing time τ.

There are limits on how weak a spin lock field strength can be used, however, since the effective fields of the two locked spins will increasingly tilt out of the transverse plane with decreasing ν. If the effective fields for spins A and B make angles of θ_A and θ_B with the z axis, chosen parallel to the static magnetic field, the cross-relaxation rate becomes:[10,14]

$$\begin{aligned}R'_{AB} &= \sin\theta_A \sin\theta_B R_{AB} \\ &\quad + \cos\theta_A \cos\theta_B R^L_{AB} \quad (19.13)\end{aligned}$$

where R_{AB} and R^{L}_{AB} are the transverse and longitudinal A–B cross-relaxation rates [cf. equations (19.6) and (19.9)]. Quantitative analysis of ROE cross-peak intensities should therefore account for the offsets and θ angles of the two spins involved. For molecules in the slow motion limit, R^{L}_{AB} and R_{AB} are of opposite sign, and θ values smaller than about 60° will seriously degrade sensitivity. In fact, if the offset and rf field strength are chosen such that the spins are aligned close to the magic angle ($\theta \approx 35^{\circ}$), the direct cross relaxation R'_{AB} will be zero in the slow tumbling limit, facilitating the study of correlated cross relaxation.[10–13]

19.5.2 HOHAHA Artifacts in ROESY

COSY artifacts of the type discussed above are easily recognized, since they yield the characteristic antiphase multiplet pattern with zero integrated intensity. A second type of magnetization transfer can occur among J-coupled spins, and yields in-phase multiplet patterns that are of the same sign as the diagonal resonances, i.e., the artifacts are of opposite sign to the true ROESY cross peaks. This so-called homonuclear Hartmann–Hahn effect (HOHAHA) occurs when the difference in effective spin lock fields, $\nu_A - \nu_B$, is not much larger than the J coupling between A and B. This effect is fully analogous to the heteronuclear Hartmann–Hahn effect, which is commonly used for cross polarization of low-γ nuclei in solids[29,30] and liquids.[31,32]

For an isolated A–B spin pair, starting with A-spin magnetization locked along the effective spin lock field, the time dependence of the HOHAHA magnetization transfer, in the absence of an ROE effect, is given by

$$\hat{A}_z \rightarrow (1 + c^2 + s^2 \cos 2qt)\hat{A}_z + s^2(1 - \cos 2qt)\hat{B}_z + \text{antiphase terms} \qquad (19.14a)$$

with

$$\left.\begin{aligned} c = \cos 2\phi, \quad s = \sin 2\phi, \quad \tan 2\phi = \frac{(1 + \cos\alpha) J_{AB}}{2(\nu_A - \nu_B)} \\ \alpha = \theta_A - \theta_B \quad 2q = 2\pi[(\nu_A - \nu_B)^2 + \tfrac{1}{4}(1 + \cos\alpha)^2 J^2_{AB}]^{1/2} \end{aligned}\right\} \qquad (19.14b)$$

In equation (19.14a), the z axes have been chosen parallel to the effective field directions of the two spins, and $\hat{A}_z$ and $\hat{B}_z$ represent the in-phase A and B spin magnetization components along their respective effective fields. The angle between the two effective fields is α. Equation (19.14) illustrates the oscillatory behavior of the HOHAHA magnetization transfer as a function of mixing time duration. Provided $|\nu_A - \nu_B| \gg J_{AB}$, the angle 2ϕ becomes very small, resulting in a vanishingly small amount of net magnetization transfer. For reliable ROESY cross-relaxation measurements involving J-coupled spins, it is therefore essential to ensure Hartmann–Hahn mismatching for J-coupled spin pairs. When the J-coupled spins A and B are very close in chemical shift and adequate Hartmann–Hahn mismatching is not possible because of the constraints imposed by equation (19.14), cross relaxation between A and a third spin X will also give rise to a spurious Hartmann–Hahn relayed ROESY cross peak between B and X.[17,33] equation (19.14), strictly speaking, only applies for an isolated pair of coupled spins. The presence of other protons, coupled to either A or B, has the effect of making the Hartmann–Hahn match condition less sharp, and requires a larger difference $|\nu_A - \nu_B|$ to ensure minimal HOHAHA contributions.[17] In practice, a reasonable compromise between minimizing the Hartmann–Hahn effects and maximizing the transverse cross relaxation is to use a spin lock rf field strength γB_2 that is at least twice as large as the width of the spectral region of interest and to position the carrier frequency on one side of the spectrum, well outside the region of interest, such that the effective field in the center of the spectrum makes an angle of about 70° with the static magnetic field. This results in an effective mismatch $|\nu_A - \nu_B| = 0.34|\delta_A - \delta_B|$, whereas, according to equation (19.13), the rate of cross relaxation is reduced by less than about 25 %. To avoid the need to use very large spectral windows and associated large data matrix sizes, the effective position of the rf carrier may be shifted just during the spin lock duration by 'phase ramping' the spin lock pulse (Figure 19.3e,f). For example, if the phase of the spin lock field is increased by 10° every m μs, this

has the effect of shifting the effective spin lock field by $10/(360m)$ MHz upfield or downfield from its original position.[10,34]

A detailed description of HOHAHA effects in ROESY has also been presented by Elbayed and Canet.[35]

19.5.3 Transverse ROESY With Minimal HOHAHA

Hwang and Shaka[36] have proposed an interesting variant of the ROESY experiment that is aimed at minimizing HOHAHA contributions. This experiment, which they refer to as transverse ROESY or T-ROESY, should not be confused with the tilted-frame T-ROESY experiment of Brüschweiler *et al.*,[10] which is aimed at measuring cross-correlation effects. In the transverse T-ROESY experiment, the mixing period consists of phase-alternated 180° pulses, applied preferably with no time between the pulses (Figure 19.3g). Near resonance, a $180^\circ_x 180^\circ_{-x}$ pulse pair has the net effect of a $4 \times (90^\circ - \theta)$ rotation about the y axis, where θ is again the angle between the effective field and the field $\boldsymbol{B}_0$. Thus, a series of $180^\circ_x 180^\circ_{-x}$ pulse pairs has the net effect of 'spin locking' along the y axis with a spin lock field that varies approximately linearly with the resonance offset frequency δ, as $2\delta/\pi$. The strong offset dependence of the Zeeman part of the Hamiltonian minimizes strong coupling effects during the mixing period, and thereby minimizes Hartmann–Hahn effects. The trajectories of the 'locked' spins during the mixing period are the same as in a rotary echo $T_{2\rho}$ experiment,[37] and the spins, on average, are aligned for equal durations along the y and z axes. As a consequence, the effective cross-relaxation rate R_{AB}(T-ROESY) is the average of the transverse cross-relaxation rate R_{AB}, equation (19.6), and the longitudinal cross-relaxation rate $R^{\mathrm{L}}_{\mathrm{AB}}$, equation (19.9). For macromolecules, the opposite signs of R_{AB} and $R^{\mathrm{L}}_{\mathrm{AB}}$ result in as much as a fourfold reduction in cross relaxation rate compared with the standard ROESY experiment, making this type of transverse ROESY experiment less effective. However, for smaller compounds, this disadvantage is less serious, and the reduction in HOHAHA effects frequently outweighs the decrease in cross relaxation rates.[38] Mixing schemes that are more elaborate than the above-mentioned $180^\circ_x 180^\circ_{-x}$ pulse pair combination have also been suggested by Hwang and Shaka,[36] but, in practice, the simpler sequence appears to yield the most reliable results.

19.6 EXAMPLES OF ROESY APPLICATIONS

A few practical examples of ROESY applications are discussed below. Figure 19.5 shows an application of the original 1D CAMELSPIN scheme to a linear tetrasaccharide. The bottom trace is the reference spectrum, obtained after a 90°_x pulse followed by a 250 ms spin lock pulse applied along the y axis. The middle spectrum represents the same experiment, preceded by a selective 180° inversion of the highest frequency (most downfield) anomeric proton at 5.1 ppm. The top spectrum shows the difference, which exhibits significant ROEs between H-1 of one sugar unit and the H-2 and H-3 protons across the interglycosidic linkage, in addition to an intraresidue ROE to its vicinal H-2 proton.

Figure 19.6 shows the application of the 2D ROESY experiment to a cyclic hexapeptide, recorded

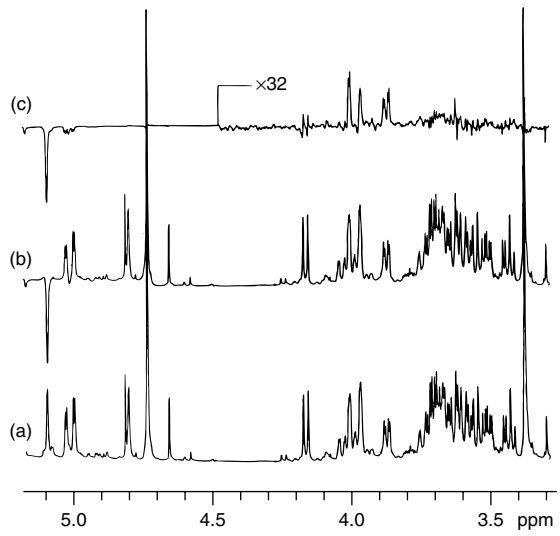

Figure 19.5. Spectra recorded with the scheme of Figure 19.3(a) for a tetrasaccharide. (a) Without selective inversion prior to the 90°_x–SL_y sequence. (b) with selective inversion of the highest frequency (most downfield) anomeric proton. (c) The difference spectrum. Positive resonances in (c) result from ROE interactions. Reprinted from Bothner-by *et al.*[5]

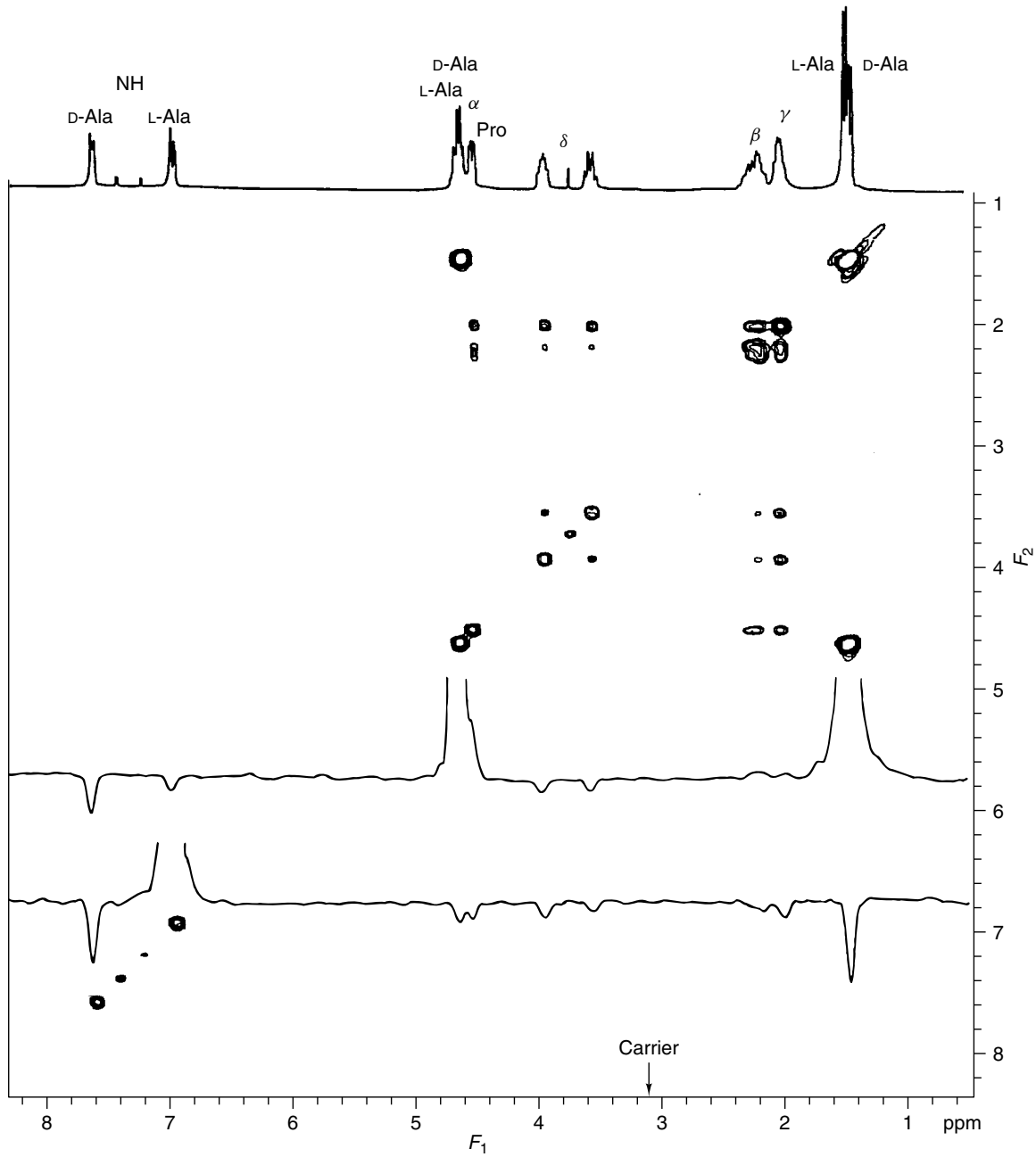

Figure 19.6. 270 MHz 2D ROESY spectrum of a cyclic hexapeptide, (D-Ala,L-Pro,L-Ala)$_2$. Only positive contour levels (for peaks with the same sign as the diagonal) are shown. The spectrum has deliberately been recorded to maximize HOHAHA contributions by positioning the carrier at 3.1 ppm and using a strong rf field strength ($\gamma B_1 = 5$ kHz) during the 200 ms spin lock. All contoured cross peaks are caused by HOHAHA transfer. The two F_1 cross sections, shown as insets, illustrate the presence of ROE cross peaks in this spectrum.

at 270 MHz ^{1}H frequency with the pulse scheme of Figure 19.3(b). In order to emphasize how serious a problem the HOHAHA may constitute, a strong (5 kHz) spin lock field was used during the mixing period and the carrier was positioned in the center of the aliphatic region, at 3.1 ppm. Only positive contour levels, of the same sign as the diagonal resonances, are shown in this figure, and all of these cross peaks are caused by spurious magnetization transfer via the HOHAHA effect. Strong HOHAHA cross peaks are seen between the H^{α} and methyl protons of both the D- and the L-Ala residues, and among all the proline protons. However, true ROE contributions are also abundant in this spectrum, as illustrated by the two insets, which represent cross sections taken at the diagonal positions of the L-Ala H^N and H^{α} resonances. The L-Ala H^N resonance, for example, shows ROE interactions with its intraresidue methyl protons, with D-Ala H^N, and with all of the proline protons. By shifting the carrier to a higher frequency position (5.1 ppm) and reducing the strength of the spin lock field to 2 kHz, the HOHAHA contributions are greatly diminished, and only two of the proline protons (H^{δ} and the H^{α} shifted most to high frequency) exhibit significant ROEs to L-Ala H^N.[18] ROE interactions to the remaining proline protons are spurious, and are relayed via HOHAHA from Pro H^{α} and Pro H^{δ} to the other ring protons.

Figure 19.7 illustrates the application of ROESY to basic pancreatic trypsin inhibitor, a 58-residue protein. This experiment was carried out in H_2O without solvent presaturation, using a water-flip-back scheme.[39,40] The figure compares F_1 cross-sections, taken at the F_2 frequency of Tyr-21 H^N, through the 2D ROESY (a) and NOESY (b) spectra. To compensate for the difference in longitudinal and transverse cross-relaxation rates, the NOESY mixing time (120 ms) was twice as long as for the ROESY experiment. Besides a slightly higher signal-to-noise ratio in the NOESY spectrum, the two cross sections exhibit some interesting differences. For example, the cross peak to Phe-45 H^N is relatively weak in the ROESY

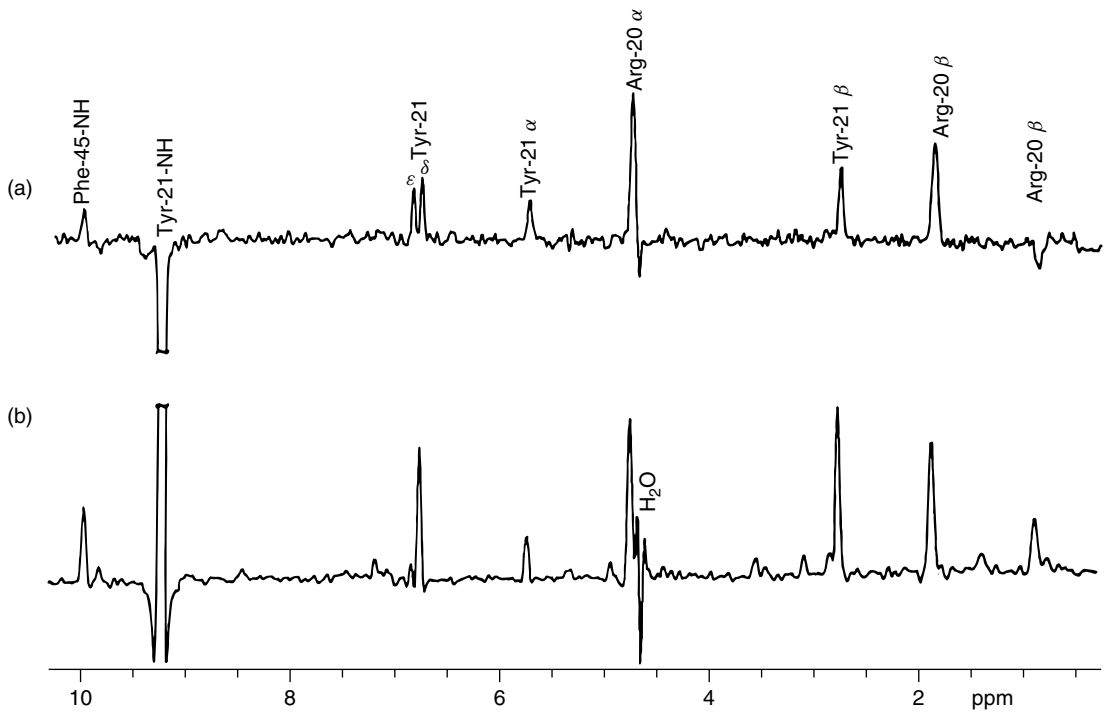

Figure 19.7. Comparison of F_1 cross sections through (a) the ROESY and (b) the NOESY spectra of BPTI, taken at the F_2 frequency of the Tyr-21 NH resonance. Both spectra were recorded at 500 MHz ^{1}H frequency under similar conditions, except for the mixing times (ROESY, 60 ms; NOESY, 120 ms). The ROESY carrier position was at 4.65 ppm and a 6.3 kHz spin lock field was used. From Bax.[17]

spectrum compared with the other cross peaks. This is due, in part, to the substantial tilt ($\theta \approx 68^\circ$) of the two spin lock fields [cf. equation (19.13)], which accounts for a loss of about 20% in the ROE build-up rate. Second, because no 90° bracketing pulses of the type shown in Figure 19.3(c) were used in this scheme, another loss of about 14% occurs (see above). Another interesting difference is seen for the Arg-20 H^β protons. Both NOESY and ROESY spectra show strong cross relaxation to the highest frequency proton of the two H^β protons, but for the low frequency H^β, the ROE cross peak is opposite in sign to the direct ROE cross peaks, indicating that it results from an indirect interaction, presumably via its geminal proton. Therefore, the NOE cross peak observed for the low frequency Arg-20 H^β proton in Figure 19.7(b) must also be caused largely by spin diffusion. The same is probably true for the other weak cross peaks observed in the NOESY cross-section, but absent in the ROESY spectrum. Finally, the backbone amide proton of Tyr-21 shows a NOE interaction to Tyr-21 H^δ, with only a very weak cross peak at the adjacent H^ϵ resonance, which is presumably due to spin diffusion. In the ROESY spectrum, the cross peaks to H^δ and H^ε are of comparable intensity, however, because the H^δ ROE cross-peak intensity is relayed efficiently to H^ϵ owing to the small $H^\delta - H^\varepsilon$ chemical shift difference and the large $H^\delta - H^\varepsilon$ J coupling.

19.7 DIFFERENT AREAS OF APPLICATION

19.7.1 Molecular Structure

Most applications of ROESY published to date deal with determination of either the primary structure, the stereochemistry, or the conformation of intermediate size molecules that show vanishingly weak laboratory frame NOEs. Because of the generally good ^1H resonance dispersion in peptides, HOHAHA effects are usually not a serious problem, and numerous applications of ROESY to the study of peptide conformation have appeared in the recent literature. Applications to the study of carbohydrate structure are also widespread, although the lack of resonance dispersion found in this class of molecules requires very careful interpretation to avoid the pitfalls of HOHAHA-relayed false ROE cross peaks. By far the largest number of literature reports on ROESY applications relates to determination of the primary structures and/or absolute configurations of natural products such as alkaloids, carotenoids, antibiotics, and other complex hydrocarbons. Interesting applications have also been reported for the study of the structure of inclusion complexes and other intermolecular interactions.

19.7.2 Macromolecular Structure

Bauer *et al*.[8] demonstrated by both computer simulation and experiment that spin diffusion effects in DNA generally pose less of a problem in ROESY spectra than in the corresponding NOESY spectra. They demonstrate, for example, that in regular B-form DNA, the ROE cross peak between the base H-6/H-8 proton and the H-1′ sugar proton of the preceding nucleotide never reaches a measurable value before it changes sign owing to the indirect three-spin effect via the vicinal H-2″ proton. Although the sequential base-to-H-1′ NOE cross peak frequently plays a key role in obtaining the sequential resonance assignments in DNA, the ROE experiment proves that it is almost entirely caused by spin diffusion, even at short mixing times, and it therefore has little value in structure calculations. Because of the absence of long-range NOE constraints in most regular types of DNA and RNA structure, it has been argued that it is essential to determine in a very precise manner the limited number of distances that can be measured, and the ROESY experiment can play an important role in this process.

In proteins, the emphasis has been on determining as many NOE interactions as possible,[21] and the value of using very precise interproton distances, or upper limits thereof, has not yet been convincingly demonstrated. Nevertheless, there are numerous situations where the ROESY experiment can provide important distance information in a sensitive manner, which can be critical for stereospecific assignment of H^β methylene protons, for example.[41] In the NOESY spectrum, the H^α protons of residues with a C^β methylene site invariably show NOE cross peaks to both H^β protons. If one of the H^β protons shows a weaker NOE to H^α than does its geminal partner, this could either be caused by the *gauche* and *trans* difference in $H^\alpha - H^{\beta 2}$ and $H^\alpha - H^{\beta 3}$ distances for a χ_1 rotamer of -60° or 180°, or by a small twist of a $\chi_1 = 60^\circ$ rotamer. In the ROESY spectrum, a *trans* ROE to a H^β methylene is never observed, since this interaction is again dominated by the three-spin effect via the

gauche H^{β} proton. If H^{α} shows positive ROEs to both H^{β} methylene protons, this indicates a χ_1 torsion angle of $+60^{\circ}$, provided that HOHAHA relay via the large geminal $^1H-^1H$ J coupling can be excluded.

19.7.3 Identification of Exchange Processes

As pointed out by Bothner-By *et al*.[5] in their original report,[5] the ROESY experiment is ideally suited for identifying chemical exchange processes that are sufficiently slow to show separate resonances for a single proton, in two or more different chemical environments, but sufficiently fast to measure magnetization transfer. The sign of the cross peak immediately discriminates between cross relaxation and chemical exchange types of magnetization transfer. In proteins and nucleic acids, cross relaxation and chemical exchange frequently occur on similar timescales, and ROESY spectra have been used extensively to identify a variety of slow exchange processes, such as aromatic ring flipping in proteins,[42,43] monomer-duplex equilibria in DNA,[44] and conformational rearrangement in a paramagnetic model heme.[45]

19.7.4 Protein Hydration

A very important application for distinguishing chemical exchange from cross-correlation effects is found in the study of protein hydration. NOE interactions between labile amide protons in a protein and the bulk water resonance are indistinguishable from hydrogen exchange. In ROESY spectra, these two effects can be conveniently distinguished by the sign of the corresponding cross peak, however.[6,7]

RELATED ARTICLES IN THE ENCYCLOPEDIA OF MAGNETIC RESONANCE

Biological Macromolecules: NMR Parameters

Peptides and Polypeptides

Polysaccharides and Complex Oligosaccharides

Protein Hydration

Relaxation Theory: Density Matrix Formulation

REFERENCES

1. J. H. Noggle and R. E. Schirmer, *The Nuclear Overhauser Effect*, Academic Press, New York, 1971.
2. J. Jeener, B. H. Meier, P. Bachmann, and R. R. Ernst, *J. Chem. Phys.*, 1979, **71**, 4546.
3. S. Macura and R. R. Ernst, *Mol. Phys.*, 1980, **41**, 95.
4. D. Neuhaus and M. Williamson, *The Nuclear Overhauser Effect in Structural and Conformational Analysis*, VCH, New York, 1989.
5. A. A. Bothner-By, R. L. Stephens, J. M. Lee, C. D. Warren, and R. W. Jeanloz, *J. Am. Chem. Soc.*, 1984, **106**, 811.
6. G. Otting and K. Wüthrich, *J. Am. Chem. Soc.*, 1989, **111**, 1871.
7. G. M. Clore, A. Bax, P. T. Wingfield, and A. M. Gronenborn, *Biochemistry*, 1990, **29**, 5671.
8. C. J. Bauer, T. A. Frenkiel, and A. N. Lane, *J. Magn. Reson.*, 1990, **87**, 144.
9. A. Bax, V. Sklenář, and M. F. Summers, *J. Magn. Reson.*, 1986, **70**, 327.
10. R. Brüschweiler, C. Griesinger, and R. R. Ernst, *J. Am. Chem. Soc.*, 1989, **111**, 8034.
11. R. Brüschweiler and R. R. Ernst, *J. Chem. Phys.*, 1992, **96**, 1758.
12. T. E. Bull, *J. Magn. Reson.*, 1987, **72**, 397.
13. T. E. Bull, in *Progress in Nuclear Magnetic Resonance Spectroscopy*, eds. J. W. Emsley, J. Feeney, and L. H. Sutcliffe, Pergamon Press, Oxford, 1992, Vol. 24, p. 377.
14. D. G. Davis, *J. Am. Chem. Soc.*, 1987, **109**, 3471.
15. B. T. Farmer II, S. Macura, L. R. Brown, *J. Magn. Reson.*, 1988, **80**, 1.
16. L. R. Brown and B. T. Farmer II, in *Methods in Enzymology*, eds. T. L. James and N. Oppenheimer, Academic Press, New York, 1989, Vol. 176, p. 199.
17. A. Bax, *J. Magn. Reson.*, 1988, **77**, 134.
18. A. Bax and D. G. Davis, *J. Magn. Reson.*, 1985, **63**, 207.
19. G. Lipari and A. Szabo, *J. Am. Chem. Soc.*, 1982, **104**, 4546.

20. G. Lipari and A. Szabo, *J. Am. Chem. Soc.*, 1982, **104**, 4559.
21. G. M. Clore, M. A. Robien, and A. M. Gronenborn, *J. Mol. Biol.*, 1993, **231**, 82.
22. D. J. States, R. A. Haberkorn, and D. J. Ruben, *J. Magn. Reson.*, 1982, **48**, 286.
23. D. Marion and K. Wüthrich, *Biochem. Biophys. Res. Commun.*, 1983, **113**, 967.
24. D. Marion, M. Ikura, R. Tschudin, and A. Bax, *J. Magn. Reson.*, 1989, **85**, 393.
25. C. Griesinger and R. R. Ernst, *J. Magn. Reson.*, 1987, **75**, 261.
26. H. Kessler, C. Griesinger, R. Kerssebaum, K. Wagner, and R. R. Ernst, *J. Am. Chem. Soc.* 1987, **109**, 607.
27. M. Rance, O. W. Sørensen, W. Leupin, H. Kogler, K. Wüthrich, and R. R. Ernst, *J. Magn. Reson.*, 1985, **61**, 67.
28. W. P. Aue, E. Bartholdi, and R. R. Ernst, *J. Chem. Phys.*, 1976, **64**, 2229.
29. S. R. Hartmann and E. L. Hahn, *Phys. Rev.*, 1962, **128**, 2042.
30. A. Pines, M. G. Gibby, and J. S. Waugh, *J. Chem. Phys.*, 1973, **59**, 569.
31. R. D. Bertrand, W. B. Moniz, A. N. Garroway, and G. C. Chingas, *J. Am. Chem. Soc.*, 1978, **100**, 5227.
32. L. Müller and R. R. Ernst, *Mol. Phys.*, 1979, **38**, 963.
33. B. T. Farmer, S. Macura, and L. R. Brown, *J. Magn. Reson.*, 1987, **72**, 347.
34. L. E. Kay, M. Ikura, R. Tschudin, and A. Bax, *J. Magn. Reson.*, 1990, **89**, 496.
35. K. Elbayed and D. Canet, *Mol. Phys.*, 1990, **71**, 979.
36. T.-L. Hwang and A. J. Shaka, *J. Am. Chem. Soc.*, 1992, **114**, 3157.
37. I. Solomon, *Phys. Rev. Lett.*, 1951, **2**, 301.
38. H. P. Wessel, B. Mayer, and G. Englert., *Carbohydr. Res.*, 1993, **242**, 141.
39. A. Bax, V. Sklenář, A. M. Gronenborn, and G. M. Clore, *J. Am. Chem. Soc.*, 1987, **109**, 6511.
40. S. Grzesiek and A. Bax, *J. Am. Chem. Soc.*, 1993, **115**, 12 593.
41. G. M. Clore, A. Bax, and A. M. Gronenborn, *J. Biomol. NMR*, 1991, **1**, 13.
42. D. G. Davis and A. Bax, *J. Magn. Reson.*, 1985, **64**, 533.
43. J. Fejzo, W. M. Westler, S. Macura, and J. L. Markley, *J. Am. Chem. Soc.*, 1990, **112**, 2574.
44. U. Schmitz, I. Sethson, W. M. Egan, and T. L. James, *J. Mol. Biol.*, 1992, **227**, 510.
45. U. Simonis, J. L. Dallas, and F. A. Walker, *Inorg. Chem.*, 1992, **31**, 5349.